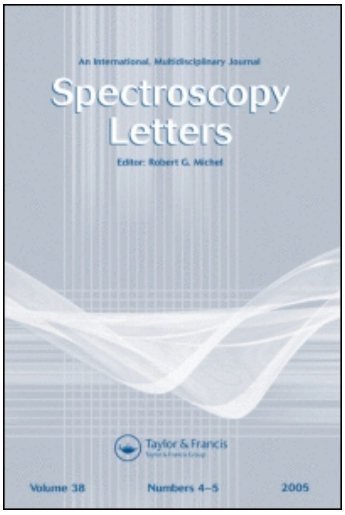


**Spectroscopy Letters**
Publication details, including instructions for authors and subscription information:
http://www.informaworld.com/smpp/title~content=t713597299

# Feasibility Study of VUV Sensitization Effect of $Tb^{3+}$

V. B. Mikhailik[a]; H. Kraus[a]
[a] Department of Physics, University of Oxford, Oxford, UK

Online publication date: 30 July 2010

**To cite this Article** Mikhailik, V. B. and Kraus, H.(2010) 'Feasibility Study of VUV Sensitization Effect of $Tb^{3+}$', Spectroscopy Letters, 43: 5, 350 — 356
**To link to this Article: DOI:** 10.1080/00387010.2010.486723
**URL:** http://dx.doi.org/10.1080/00387010.2010.486723

*Spectroscopy Letters*, 43:350–356, 2010

ISSN: 0038-7010 print/1532-2289 online
DOI: 10.1080/00387010.2010.486723

Taylor & Francis
Taylor & Francis Group

# Feasibility Study of VUV Sensitization Effect of $Tb^{3+}$

**V. B. Mikhailik and H. Kraus**

Department of Physics, University of Oxford, Oxford, UK

**ABSTRACT** The possibility to use $Tb^{3+}$ as luminescence sensitizer for enhancement of the conversion efficiency of vacuum-ultraviolet (VUV) radiation into visible light was examined. We studied the luminescence properties of $K_3Tb(PO_4)_2$ and $Ba_3Tb(PO_4)_3$ activated by $Eu^{3+}$, and of $SrAl_{12}O_{19}$ co-doped with $Mn^{2+}$ and $Tb^{3+}$ at excitation over the 120 to 300 nm wavelength range. It is shown that $Tb^{3+}$ ions, exhibiting a strong absorption band in the VUV, can provide efficient sensitization of $Eu^{3+}$ and $Mn^{2+}$ emissions for excitation in this spectral range, giving rise to intense red and green luminescence, respectively. This study provides a proof for the concept of VUV sensitization, which enables the engineering of luminescence materials with improved efficiency for excitation from a noble gas discharge.

**KEYWORDS** Tb-Eu energy transfer, Tb-Mn energy transfer, VUV phosphors, VUV sensitization



## INTRODUCTION

Phosphors are widely used for the conversion of electromagnetic emission with wavelengths shorter than that of visible light into radiation within the visible range. Prominent examples are displays, lighting devices, and visual detectors. The most efficient phosphors are realised using luminescent ions, such as Ce, Eu, Tb, and Mn, exhibiting high quantum yield when excitation falls within their characteristic absorption bands. However, a mismatch between the wavelength band of the excitation radiation and the absorption band is a more usual scenario, leading to weak absorbance and low conversion efficiency. A common way to mitigate this problem is using a strongly absorbing agent (this can be either a co-dopant or a constitutive element of the host matrix) that can transfer the excitation energy to the luminescent ion. In such a case, it is possible to achieve direct energy transfers from the more readily accessible excited state of the absorber to the emitting level of the luminescent ion. This leads to a large increase in luminescence intensity and is generally known as a sensitization effect. A classic example is the energy transfer between $Ce^{3+}$-$Tb^{3+}$ and $Gd^{3+}$- $Eu^{3+}$ pairs. The ions of the sensitizer ($Ce^{3+}$ or $Gd^{3+}$) efficiently absorb light emitted by a low-pressure mercury discharge and transfer the energy to the activator ($Tb^{3+}$ or $Eu^{3+}$), resulting in emission characteristic of these ions.

Received 30 June 2009; accepted 5 August 2009.

Address correspondence to V. B. Mikhailik, Department of Physics, University of Oxford, DWB, Keble Road, Oxford OX1 3RH, UK. E-mail: vmikhai@hotmail.com

Studies of this effect have led to the development of highly efficient phosphors, widely used in modern fluorescent lamps.[1]

While the conversion efficiency of the UV radiation of some modern phosphors is approaching the theoretical limit, there is a need for substantial improvement when VUV excitation is considered. This issue has been addressed extensively over the past decade and much effort was committed to the investigation of the quantum cutting effect.[2,3] Although quantum cutting was studied in many systems,[4–9] and research activity still continuing, no practical VUV phosphor based on this effect has been found.

## BASICS OF CONCEPT

The idea to use sensitization for the enhancement of the conversion efficiency in the VUV region is fairly straightforward. However, not many studies aiming to enhance the efficiency of the VUV-to-visible conversion using a suitable pair of co-activator ions have been successful so far. This is because the majority of hosts absorb in this spectral region and hence the classic sensitization, as a process of energy transfer from the excited sensitizer to the emitting level of the activator ion, has vanishingly low probability. Fortuitously the quest for materials for application in the VUV resulted in the characterization of many wide-gap oxides that can be used as suitable hosts for VUV sensitization. Furthermore, investigations of the spectroscopic properties of rare-earth (RE) ions in the high energy range[10,11] provided important information that is needed for engineering VUV phosphors, utilizing sensitization for emission enhancement. Having all this information available, it was natural to suggest that $Tb^{3+}$, exhibiting a strong $4f^7\ 5d$ absorption band in the VUV, should provide a sensitization effect at excitation in this energy range.

The main requirement for sensitization is the availability of an efficient energy transfer between the terbium ion as sensitizer and the relevant activator. To investigate the feasibility of this concept, $Eu^{3+}$ and $Mn^{2+}$ were selected as acceptor ions. The energy transfer from the $^5D_3$, $^5D_4$ levels of $Tb^{3+}$ to the $^5D_1$ level of $Eu^{3+}$ has long been established,[12,13] and it has also been demonstrated that it is particularly efficient in phosphates.[13,14] The energy transfer process from $Tb^{3+}$ to $Mn^{2+}$ has also been demonstrated in aluminate hosts.[15] To allow efficient energy transfer to the activator ion at VUV excitation, the host matrix should satisfy several requirements. The material should be transparent in the energy range of the $4f^7\ 5d$ absorption transitions of $Tb^{3+}$. A strong host absorption band above the absorption bands of $Tb^{3+}$ can be advantageous for excitations at higher energies. Finally, since there is generally a gap between the energy levels of sensitizer ($Tb^{3+}$) and selected activator ions that needs to be bridged by emission or absorption of phonons, the hosts with a high frequency of internal vibrations are preferable. The analysis of published data shows that the RE-based phosphates with a $PO_4$ group, which absorb photons of energy $>7$ eV[16] and exhibit internal vibration modes with a high frequency,[13] should satisfy these conditions. This motivated the choice of the potassium rare-earth double phosphate $K_3Ln(PO_4)_2$ (Ln stands for RE-ion) and barium rare-earth orthophosphate $Ba_3Ln(PO_4)_3$ as hosts to study the effect of the sensitization of the $Eu^{3+}$ emission.

To study sensitization of $Mn^{2+}$ emission by $Tb^{3+}$ we have chosen strontium aluminate $SrAl_{12}O_{19}$ which is an excellent wide band gap phosphor[1,17] The structure of this compound permits accommodation of the large rare earth ions of $Tb^{3+}$ in the 12-fold coordination position of $Sr^{2+}$, while transition metal ions of $Mn^{2+}$ can substitute $Al^{3+}$ in the tethraedral coordination.[17] Furthermore, the layered structure of the host, which results in a less pronounced concentration quenching of the luminescence, is an additional advantage as this permits experimenting with relatively high levels of doping.

## EXPERIMENTAL PROCEDURES

The experimental samples that have been used in this study were synthesized from a mixture of high-purity raw materials, using a conventional solid-state reaction technique. It includes thorough mixing of the powder materials under hexane and preheating to 600°C in air to decompose carbonates. Then the mixture was pulverized again and fired for 6 hours on air at temperature 1300°C (phosphates) or 1450°C (aluminates). Gadolinium is known to be an efficient sensitizer of the $Eu^{3+}$ emission at UV excitation.[1] Therefore, to study the sensitization

effect of the $Tb^{3+}$ in Eu-doped phosphates, we have used Gd-based analogs for comparison purposes. To study the effect of $Tb^{3+}$ on the emission of the $Mn^{2+}$ radiation, we have used samples of $SrAl_{12}O_{19}$, solely doped with $Mn^{2+}$ and $Tb^{3+}$ and also co-doped with $Mn^{2+}$ and $Tb^{3+}$. The structure of the samples was verified using powder X-ray diffraction. The luminescence characterization of the phosphors has been carried out at the SUPERLUMI station of HASYLAB, which is designed for comprehensive investigations of luminescence materials in the VUV range.[18] The phosphor samples, prepared as pellets of the same dimensions, were glued to the sample holder of a He-flow cryostat using silver conductive paint. The excitation spectra were recorded with a PMT (Hamamatsu, R6358P), while the emission spectra were measured with higher resolution by means of a liquid nitrogen cooled CCD camera (Princeton Instruments) mounted on the second exit arm of a SpectraPro308 (Action Research) monochromator. During the measurements, different samples were presented to the excitation radiation by translating the holder in a direction orthogonal to the beam. This ensured that the same geometry was established for light collection from different samples, thereby allowing comparison of the luminescence emitted.



# RESULTS

## Emission Spectra

The room temperature emission spectra of the Eu-doped $K_3Tb(PO_4)_2$ and $K_3Gd(PO_4)_2$, samples, measured at 150 nm excitation, are displayed in Fig. 1a. The luminescence spectra of the $K_3Tb_{0.9}Eu_{0.1}(PO_4)_2$ exhibit the characteristic red emission of $Eu^{3+}$ due to the $^5D_0 \rightarrow {}^7F_j$ transitions that prevails over the Tb $4f^n$-$4f^n$ emission (the characteristic lines at 490 and 540 nm). The $Eu^{3+}$ emission also dominates the luminescence spectrum of the $K_3Gd_{0.9}Eu_{0.1}(PO_4)_2$; only a weak $Gd^{3+}$ line ($^6P_{7/2} \rightarrow {}^8S_{7/2}$ transition) is detected at 312 nm. This indicates the efficient energy transfer from the host to $Eu^{3+}$ in these phosphors. It is worthwhile to remark that the integrated intensity of the $K_3Tb_{0.9}Eu_{0.1}(PO_4)_2$ under 150 nm excitation is significantly higher (by a factor of 8) compared with that of a Gd-based analog. The emission intensity of the $K_3Tb_{1-x}Eu_x(PO_4)_2$ decreases monotonously with increasing concentration of europium; the highest intensity at room temperature was observed for the sample with $x = 0.05$.

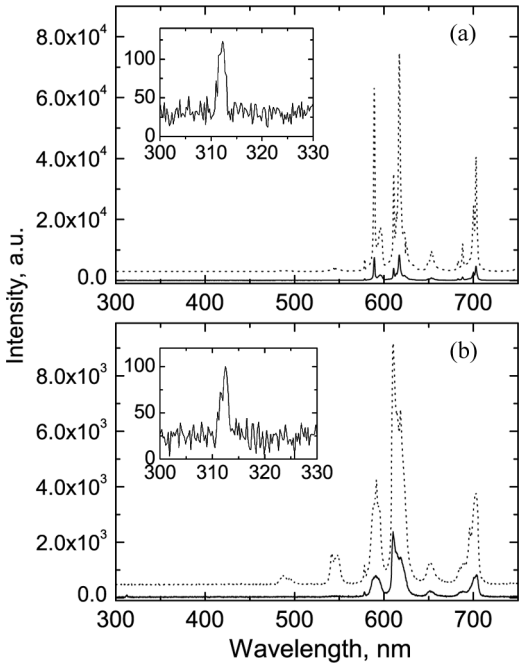


**FIGURE 1** **(a) Luminescence spectra of the $K_3Tb_{0.9}Eu_{0.1}(PO_4)_2$ (dots) and $K_3Gd_{0.9}Eu_{0.1}(PO_4)_2$ (line). (b) Luminescence spectra of $Ba_3Tb_{0.9}Eu_{0.1}(PO_4)_3$ (dots) and $Ba_3Gd_{0.9}Eu_{0.1}(PO_4)_3$ (line). Spectra are recorded for 150 nm excitation at T = 295 K. The insets show the range of the luminescence spectra of $K_3Gd_{0.9}Eu_{0.1}(PO_4)_2$ and $Ba_3Gd_{0.9}Eu_{0.1}(PO_4)_3$ with $Gd^{3+}$ emission.**

Figure 1b shows the luminescence spectra of the two phosphors $Ba_3Tb_{0.9}Eu_{0.1}(PO_4)_3$ and $Ba_3Gd_{0.9}Eu_{0.1}(PO_4)_3$ measured at room temperature under excitation with 150 nm photons. The principal features of the emission spectra are very similar to those observed in Eu-doped potassium rare-earth double phosphates: $Eu^{3+}$ emission dominates the luminescence spectrum whereas the intensities of the $Tb^{3+}$ and the $Gd^{3+}$ $4f^n$-$4f^n$ lines are much weaker than that of the $Eu^{3+}$. As is mentioned above, such features of the emission spectra signify the energy transfer to $Eu^{3+}$. Results show that the $Eu^{3+}$ emission intensity in the $Ba_3Tb_{0.9}Eu_{0.1}(PO_4)_3$-Eu under 150 nm excitation is enhanced fivefold, compared with $Ba_3Gd_{0.9}Eu_{0.1}(PO_4)_3$.

Figure 2 shows the room temperature luminescence spectra of the $SrAl_{12}O_{19}$ doped with $Tb^{3+}$ and $Mn^{2+}$. At high-energy excitation ($\lambda = 150$ nm) the $SrAl_{12}O_{19}$-Mn exhibits an asymmetric emission band with a maximum at 515 nm, attributed to the $^4T_{1g}$-$^6A_{1g}$ transitions of the $Mn^{2+}$ ions that occupy the trahedral positions in the lattice. The luminescence spectrum of $SrAl_{12}O_{19}$-Tb exhibits characteristic

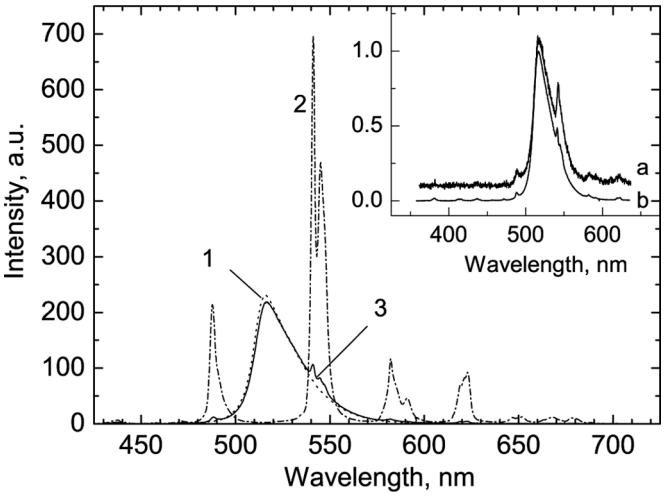


**FIGURE 2** **Luminescence spectra of 1 – $SrAl_{12}O_{19}$-Mn (20 at.%), 2 – $SrAl_{12}O_{19}$-Tb (20 at.%) and 3- $SrAl_{12}O_{19}$-Mn (10 at.%), Tb (10 at.%) measured at 150 nm excitation. T = 295 K. The inset displays the normalised luminescence spectra of $SrAl_{12}O_{19}$-Mn(10 at.%), Tb (10 at.%) measured at 215 (a) and 150 nm (b) excitation.**

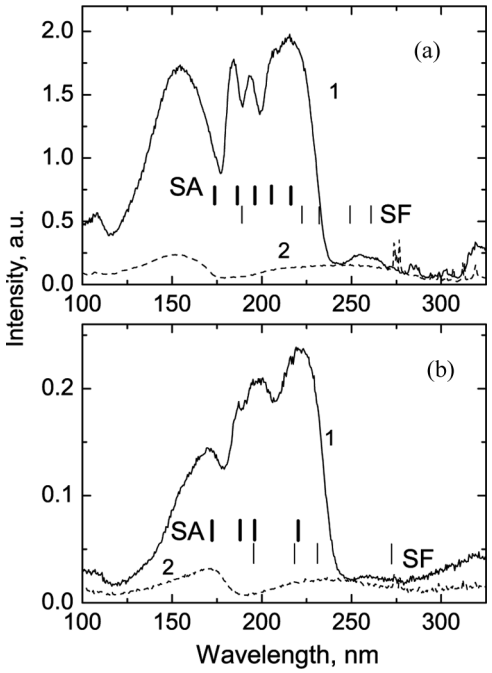


**FIGURE 3** **(a) Excitation spectra of $K_3Tb_{0.9}Eu_{0.1}(PO_4)_2$ (1) and $K_3Gd_{0.9}Eu_{0.1}(PO_4)_2$ (2). (b) Excitation spectra of $Ba_3Tb_{0.9}Eu_{0.1}(PO_4)_3$ (1) and $Ba_3Gd_{0.9}Eu_{0.1}(PO_4)_3$ (2). Spectra are monitored at 610 nm at T = 295 K. Vertical bars show the calculated positions of $Tb^{3+}$ bands.**

emission lines, associated with the *f-f* transitions in $Tb^{3+}$. It is clearly seen that in the luminescence spectrum of the samples co-doped with $Mn^{2+}$ and $Tb^{3+}$, the emission band of manganese dominates whereas $Tb^{3+}$ emission is strongly suppressed.

Only a small peak is observed around 541 nm at the long-wavelength side of the $Mn^{2+}$ emission band. It should be noted that the $Mn^{2+}$ emission band remains dominant in the luminescence spectrum of $SrAl_{12}O_{19}$-Mn, Tb when the phosphor is excited above 200 nm (see inset in Fig. 2). In this region the excitation efficiency of $Mn^{2+}$ is very poor and mainly the $Tb^{3+}$ ions are excited through the $4f^8 \rightarrow 4f^7\ 5d$ transitions. This provides evidence of the energy transfer process from $Tb^{3+}$ to $Mn^{2+}$, consistent with recent studies of $LaMgAl_{11}O_{19}$-Tb, Mn.[15]

## Excitation Spectra

The excitation spectra for Eu-emission in the phosphates under investigation are shown in Fig. 3. The UV part of the excitation spectrum of $K_3Gd(PO_4)_2$-Eu and $Ba_3Gd_{0.9}Eu_{0.1}(PO_4)_3$-Eu, monitored at the maximum of the $Eu^{3+}$ emission, shows a manifold of sharp peaks associated with the $4f^n$-$4f^n$ intraconfiguration transitions in $Eu^{3+}$ and $Gd^{3+}$. A broad band at 235 nm is due to charge transfer transitions between the oxygen ligand and $Eu^{3+}$. A high-energy band at 155 ($K_3Gd(PO_4)_2$-Eu) and 170 nm ($Ba_3Gd_{0.9}Eu_{0.1}(PO_4)_3$-Eu) should be attributed to the excitation of the host matrix in the absorption region of the $PO_4$ groups since the lowest transition energy of the tetrahedral $PO_4$ molecule is located at 7 to 10 eV.[16,19,20]

It was found that the excitation spectra of $Tb^{3+}$ and $Eu^{3+}$-emissions of $K_3Tb(PO_4)_2$-Eu are very similar,[21] thus providing clear evidence of excitation of $Eu^{3+}$ ions by means of energy transfer from terbium. The excitation spectrum consists of a short-wavelength (150 nm) band, assigned to the host lattice absorption and three intense long-wavelength bands that can be attributed to the spin-allowed (SA) $4f^8 \rightarrow 4f^7\ 5d$ transitions of $Tb^{3+}$ ions.[10,11] Due to crystal field splitting of the excited energy levels, the spectra are composed of several bands. In addition to the spin-allowed (SA) transitions much weaker bands associated with the spin-forbidden (SF) transitions can also be seen in the low-energy part of the excitation spectra at $\lambda > 240$ nm. The occurrence of the spin-dependant transitions is the result of a change of the spin orientation and hence multiplicity of the excited state.

The excitation spectrum of $Ba_3Tb_{0.9}Eu_{0.1}(PO_4)_3$, monitored at 610 nm, consists of the overlapping bands between 180 and 240 nm and a separate band

due to the absorption of the host lattice at 170 nm. The structure of the excitation spectra between 180 and 240 nm can be interpreted as the spin-allowed $4f^8 \rightarrow 4f^7\ 5d$ transitions of the $Tb^{3+}$ ions. Although theory predicts five levels associated with these transitions in terbium, the energy difference between the $4f^7\ 5d$-levels is controlled by the effect of crystal field splitting. Since the $Ba_3Tb(PO_4)_3$ matrix exhibits cationic disorder,[22] the local crystal field at the $Tb^{3+}$ ion varies, which in turn causes a broadening of the $4f^7\ 5d$-bands and their overlap. Because of this, some of the bands of interest can not be resolved. It should be noted, that the same applies to $4f \rightarrow 5d$ transitions of $Ce^{3+}$ that should split into five crystal field levels, while recent studies have enabled to identify only four principal bands in the excitation spectra of $Ba_3Ce(PO_4)_3$.[23]

Figure 4 shows the excitation spectra of the strontium aluminate phosphors. The $SrAl_{12}O_{19}$-Mn exhibits strong excitation bands below 200 nm (155 and 180 nm). Given the value of the band gap (7.5 eV) the former band is assigned to valence-conduction band transitions of the crystal. The band at 180 nm can be tentatively attributed either to charge-transfer transition in which the $Mn^{2+}$ is involved or to the $Mn^{2+} \rightarrow Mn^{3+}$ auto-ionisation. The absorption above 200 nm is due to the $3d^5 \rightarrow 3d^4\ 4s$ transition from the ground to excited states of $Mn^{2+}$.

The excitation spectrum of the Tb-doped sample consists of two intense bands at 165 and 190 nm as well as less intense peaks at 182, 202, 208, and 216 nm. We attribute the first band to the absorption of the host lattice that overlaps with the charge-transfer absorption of $Tb^{3+}$-$O^{2-}$. Other peaks are due to the interconfiguration $4f^8 \rightarrow 4f^7\ 5d$ transitions of $Tb^{3+}$.[24] The broad bands are assigned to the SA *fd* transitions while much weaker bands at the low-energy side of the excitation spectra are associated with the SF transitions.

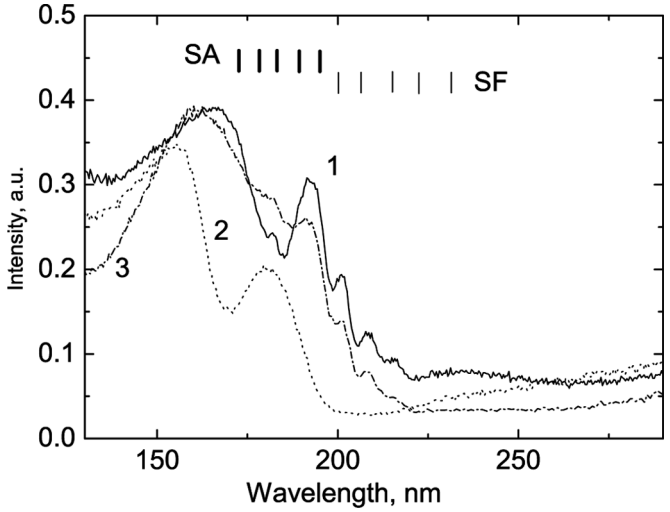


**FIGURE 4** Excitation spectra of 1 – $SrAl_{12}O_{19}$-Tb 0.2 ($\lambda_{em}$ = 541 nm), 2 – $SrAl_{12}O_{19}$-Mn0.2. ($\lambda_{em}$ = 515 nm), 3 – $SrAl_{12}O_{19}$-Mn0.1Tb0.1 ($\lambda_{em}$ = 515 nm). T = 295 K. Vertical bars show the calculated positions of $Tb^{3+}$ bands.

As can be seen from Fig. 4 the excitation spectrum of the $SrAl_{12}O_{19}$-Mn (10 at %) Tb (10 at %), monitored at 515 nm, shows a broad band at 160 nm and a clear shoulder-like structure at 182, 191, 202 208 and 216 nm, that is, apparently, absent in the excitation spectra of the Mn-doped sample. Furthermore, the excitation spectrum of the $Tb^{3+}$ emission monitored at 541 nm was found to be very similar to the excitation spectrum of the $Mn^{2+}$ emission in this sample. This finding clearly demonstrates that $Mn^{2+}$ is excited both directly and via energy transfer from $Tb^{3+}$. The excitation spectrum in the 160 to 180 nm range is due to the superposition of the overlapping $Tb^{3+}$ and $Mn^{2+}$ bands while the structure below 150 nm, which is common for all samples, is due to the excitation of the host lattice.

## DISCUSSION

The general features of the luminescence excitation spectra in the $Tb^{3+}$-doped compounds can be interpreted using methodology developed by Dorenbos.[11] This approach allows to predict the position of the $4f^{n-1}\ 5d$ energy levels of RE ions, using that observed for $Ce^{3+}$ in the same compound. In the context of this empirical shift model the energies of the SA *fd* transitions of $Tb^{3+}$ can be constructed by adding a constant value $\lambda E = 1.66 \pm 0.12$ eV to the energies of the $4f5d$ transitions of $Ce^{3+}$, observed in the same host. The energies of the SF transitions can be generated by applying a shift of −1 eV to the energy of the SA transitions of the $Tb^{3+}$. This approach was used to obtain the positions of the $Tb^{3+}$ bands in $K_3Tb(PO_4)_2$, using the published data on the spectroscopy of $Ce^{3+}$ in the $K_3La(PO_4)_2$.[25] The first two SF bands of $Tb^{3+}$ (253 and 261 nm, see Fig. 3a) are predicted well. The strong band between 200 and 240 nm comprises both the SA and the SF transitions that contribute to the observed structure of the band. It is known

that the SF transitions can be sensibly intense in a low symmetry crystal field. This is the case here, as the $Tb^{3+}$ ion occupies a low-symmetric seven-fold coordinated position in the $K_3Tb(PO_4)_2$.[26] Furthermore, as is stated in,[11] the intensity of the $Tb^{3+}$ SF excitation bands has a tendency of becoming stronger at higher energies. The assignment of the positions of the high energy band at 182 and 191 nm is less successful since the calculated positions for these peaks are located at larger than expected wavelengths.

The shift model was applied to calculate the energy of the spin allowed $4f^8 \rightarrow 4f^7\ 5d$ transitions of the $Tb^{3+}$ in $Ba_3Tb_{0.9}Eu_{0.1}(PO_4)_3$. Using the peak positions of the main excitation bands of $Ce^{3+}$ in $Ba_3Ce(PO_4)_3$ (320, 270, 250 and 220 nm[23]), we found that the $4f^7\ 5d$ bands of $Tb^{3+}$ in the $Ba_3Tb_{0.9}Eu_{0.1}(PO_4)_3$ should be observed at 224, 198, 187 and 170 nm. Reassuringly, this finding is supported by the experimental data: all bands peak very close to the calculated positions (see Fig. 3b).

It is worthwhile to remark that, according to the model, the short-wavelength band of $Tb^{3+}$ merges with the continuum of the valence to conduction band transitions of the $PO_4$ group in both phosphate phosphors. This creates favorable conditions for the energy transfer from the $PO_4$ group to the Tb ions, explaining hereby the enhanced efficiency of the phosphors at excitation in this energy range.

Using these results, we constructed the energy diagram and the scheme of energy transfer processes in Eu-Tb co-doped phosphates (Fig. 5). According to this scheme, the VUV radiation is absorbed by the terbium ions in the course of the allowed $4f^8 \rightarrow 4f^7\ 5d$ transitions. The excitations quickly relax, populating the lowest emitting levels of the $Tb^{3+}$ and then they are transferred to the $Eu^{3+}$. The final stage of the relaxation process, i.e., the *f-f* transition of $Eu^{3+}$, results in emission in the red. The energy transfer process is not fully efficient and therefore $Tb^{3+}$ *f-f* emission is also observed.

Finally, we applied the shift model to derive the positions of the $Tb^{3+}$ bands in $SrAl_{12}O_{19}$. It was shown that the calculated positions of the transitions relate reasonably well to the main features of the excitation spectrum. The positions of all but one SF bands are identified very well; only the first band is rather diffuse and cannot be determined accurately. The strongest band, observed at 191 nm, can be

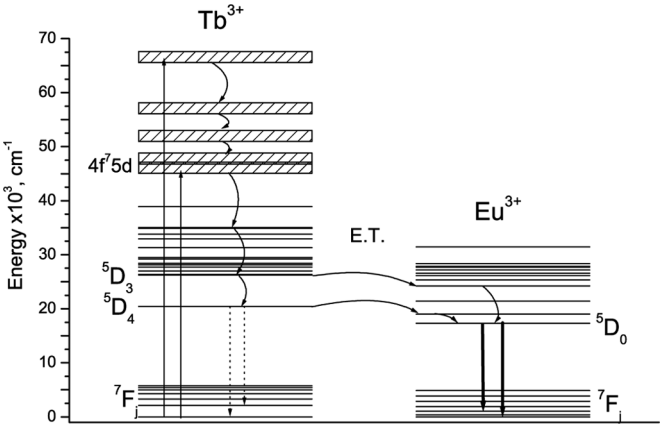


**FIGURE 5** **Energy level diagram of a Tb-Eu-doped phosphor and scheme of transitions involved in the luminescence process.**

attributed to two overlaping SA bands peaking at 193 and 188 nm (see Fig. 4). The third SA band at 183 nm is also predicted well. The assignment of the positions of the high energy bands is less successful since they cannot be identified in the excitation spectrum. We suppose that they merge with the much stronger charge transfer band $Tb^{3+}$-$O^{2-}$.

Figure 6 displays the energy level diagram of the $Tb^{3+}$-$Mn^{2+}$ co-doped phosphor and possible radiative transitions. Generally, the mechanism of the process involved is very similar to that highlighted in the $Tb^{3+}$-$Eu^{3+}$ co-doped phosphor. The excitation energy is absorbed by the $Tb^{3+}$ ions, relaxes and transfers to the $Mn^{2+}$ ions, so the only essential difference is the final emission stage that occurs in the $Mn^{2+}$ generating green emission. It is also worth to remark, that the light produced by the $Tb^{3+}$-$Mn^{2+}$ pair remains suitable for applications that require high color purity because of the overlap of the main emission bands of both luminescent ions.

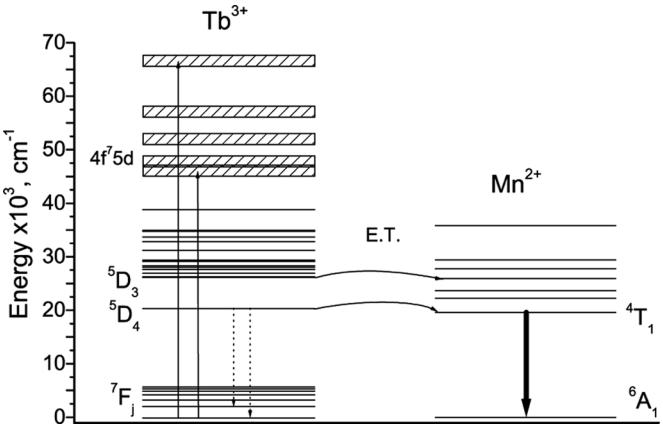


**FIGURE 6** **Energy level diagram of a Tb-Mn co-doped phosphor and scheme of transitions involved in the luminescence process.**

## CONCLUSION

The need for more efficient and environmentally friendly methods of generating visible light calls for the development of innovative concepts. We examined the prospect of VUV sensitization as a possible way to enhance the conversion efficiency of high-energy VUV radiation from a noble gas discharge source into visible light. Our study clearly demonstrates the feasibility of VUV sensitization of the $Eu^{3+}$ emission by $Tb^{3+}$ ions in phosphate hosts. The $K_3Tb(PO_4)_2$-Eu and the $Ba_3Tb_{0.9}Eu_{0.1}(PO_4)_3$ exhibit significant (a few times) improvement of the light output compared with Gd-based analogs.

We also investigated the VUV-excited luminescence of $SrAl_{12}O_{19}$, co-doped with $Tb^{3+}$ and $Mn^{2+}$ and observed a sensitization effect in this system. Though the total emission intensity of the $Tb^{3+}$ and $Mn^{2+}$ co-doped phosphor shows no noticeable enhancement compared with the $Mn^{2+}$ doped analog, we hope that this can be improved by tuning the concentrations of the co-dopants.

An additional merit of VUV sensitization by means of $Tb^{3+}$ ions in all phosphors under study is the manifestation of a strong excitation band at 160 nm. This allows better utilization of the broad band emission from a noble gas discharge. Altogether, the results of these studies show that the VUV sensitization effect in Tb-Eu and Tb-Mn co-doped systems can open real possibilities for the creation of more efficient VUV phosphors.



## ACKNOWLEDGMENT

The research leading to these results has received funding from the European Community's Seventh Framework Programme (FP7/2007–2013) under grant agreement No. 226716.

## REFERENCES


1. Shionoya, S.; Yen, W. M. Eds. *Phosphor Handbook*; CRC Press: Boca Raton, FL, 1999; 921.
2. Wegh, R.; Donker, H.; Meijerink, A.; Lamminmaki, R. J.; Holsa, J. Vacuum-ultraviolet spectroscopy and quantum cutting for $Gd^{3+}$ in $LiYF_4$. *Phys. Rev. B* **1997**, *56*, 13841–13848.
3. Ronda, C. Luminescent materials with quantum efficiency larger than 1, status and prospects. *J. Lumin.* **2002**, *100*, 301–305.
4. Srivastava, A. M.; Beers, W. W. Luminescence of $Pr^{3+}$ in $SrAl_{12}O_{19}$ Observation of two photon luminescence in oxide lattice. *J. Lumin.* **1990**, *71*, 285–290.
5. van der Kolk, E.; Dorenbos, P.; Vink, A. P.; Perego, R. C.; van Eijk, C. W. E.; Lakshmanan, A. R. Vacuum ultraviolet excitation and emission properties of $Pr^{3+}$ and $Ce^{3+}$ in $MSO_4$ ($M$ = Ba, Sr, and Ca) and predicting quantum splitting by $Pr^{3+}$ in oxides and fluorides. *Phys. Rev. B* **2001**, *64*, 195129.
6. Kodama, N.; Watanabe, Y. Visible quantum cutting through downconversion in $Eu^{3+}$-doped $KGd_3F_{10}$ and $KGd_2F_7$ crystals. *Appl. Phys. Lett.* **2004**, *84*, 4141–4143.
7. Moine, B.; Beauzamy, L.; Gredin, P.; Wallez, G.; Labeguerie, J. Research of green emitting rare-earth doped materials as potential quantum-cutter. *Opt. Mater.* **2008**, *30*, 1083–1087.
8. Zhou, Y.; Feofilov, S. P.; Seo, H. J.; Jeong, J. Y.; Keszler, D. A.; Meltzer, R. S. Energy transfer to $Gd^{3+}$ from the self-trapped exciton in $ScPO_4$:$Gd^{3+}$: Dynamics and application to quantum cutting. *Phys. Rev. B* **2008**, *77*, 075129.
9. Hachani, S.; Moine, B.; El-akrmi, A.; Férid, M. Luminescent properties of some ortho- and pentaphosphates doped with $Gd^{3+}$–$Eu^{3+}$: Potential phosphors for vacuum ultraviolet excitation. *Opt. Mater.* **2009**, *31*, 678–684.
10. van Pieterson, L.; Reid, M. F.; Burdick, G. W.; Meijerink, A. $4f^n \rightarrow 4f^{n-1}$ 5*d* Experiment and theory transitions of the heavy lanthanides. *Phys. Rev. B* **2002**, *65*, 045114.
11. Dorenbos, P. Exchange and crystal field effects on the $4f^{n-1}5d$ levels of $Tb^{3+}$. *J. Phys.: Cond. Matter* **2003**, *15*, 6249–6268.
12. Holloway, W. W.; Kestigian, J. M.; Newman, R. Direct evidence for energy transfer between rare earth ions in terbium-europium tungstates. *Phys. Rev. Lett.* **1963**, *11*, 458–460.
13. Laulicht, I.; Meirman, S. Direct evidence for excitation transfer from $^5D_4$ manifold of $Tb^{3+}$ to $^5D_1$ manifold of $Eu^{3+}$ in $Tb_{0.66}Eu_{0.33}P_5O_4$. *J. Lumin.* **1986**, *34*, 287–293.
14. Schierning, G.; Batentschuk, M.; Osvet, A.; Winnacker, A. On the energy transfer from $Tb^{3+}$ to $Eu^{3+}$ in $LiTb_{1-x}Eu_xP_4O_{12}$. *Rad. Measure.* **2004**, *38*, 529–532.
15. You, H.; Song, Y.; Jia, G.; Hong, G. Energy transfer from $Tb^{3+}$ to $Mn^{2+}$ in $LaMgAl_{11}O_{19}$:Tb, Mn phosphors. *Opt. Mate.* **2008**, *31*, 342–345.
16. Mishra, K. C.; Osterloh, I.; Anton, H.; Hannebauer, B.; Schmidt, P. C.; Johnson, K. H. First principles investigation of host excitation of $LaPO_4$, $La_2O_3$ and $AlPO_4$. *J. Lumin.* **1997**, *72–74*, 144–145.
17. Verstegen, J. M. P. J.; Stevels, A. L. N. The relation between crystal structure and luminescence in β-alumina and magnetoplumbite phases. *J. Lumin.* **1974**, *9*, 406–414.
18. Zimmerer, G. SUPERLUMI: A unique setup for luminescence spectroscopy with synchrotron radiation. *Rad. Measure.* **2007**, *42*, 859–864.
19. Nakazawa, E.; Shiga, F. Vacuum ultraviolet luminescence excitation spectra of $RPO_4$:$Eu^{3+}$ (R=Y, Ln, Gd and Lu). *J. Lumin.* **1977**, *15*, 255–259.
20. Saito, S.; Wada, K.; Onaka, R. Vacuum ultraviolet reflection spectra of KDP and ADP. *J. Phys. Soc. Japan* **1974**, *37*, 711–715.
21. Mikhailik, V. B.; Kraus, H.; Dorenbos, P. Efficient VUV sensitization of $Eu^{3+}$ emission by $Tb^{3+}$ in potassium rare-earth double phosphate. *Physica Status Solidi RRL* **2009**, *1*, 13–15.
22. Barbier, J. Structural refinements of eulytite-type $Ca_3Bi(PO_4)_3$ and $Ba_2La(PO_4)_3$. *J. Solid State Chem.* **1992**, *101*, 249.
23. Liang, H. B.; Tao, Y.; Su, Q. The luminescence properties of $Ba_3Gd_{1-x}Ln_x(PO_4)_3$ under synchrotron radiation VUV excitation. *Mate. Sci. Eng. B* **2005**, *119*, 152–158.
24. Dorenbos, P. 5-d level energies of Ce3+ and the crystalline environment. IV Aluminates and ''simple'' oxides. *J. Lumin.* **2002**, *99*, 283–299.
25. Finke, B.; Shwartz, L.; Gürtler, P.; Krass, M. Optical properties of potassium rare earth orthophosphates (RE = La, Ce, Tb). *Physica Status Solidi A* **1992**, *130*, K125–K128.
26. Boatner, L. A.; Keefer, L. A.; Farmer, J. M.; Wisniewski, D.; Wojtowicz, A. J. Cerium-activated rare-earth orthophosphate and double-phosphate scintillators for x- and gamma-ray detection. *Proc. SPIE* **2004**, *5540*, 73–86.